Revue des Composites et des Matériaux Avancés-Journal of Composite and Advanced Materials
Vol. 36, No. 2, April, 2026, pp. 281-292
Journal homepage: http://iieta.org/journals/rcma

Failure Prediction of Brick–Recycled Aggregate Composite Walls Under Blast Loading Using Finite Element Analysis

Ali Ghalib[1*], Zainab Sharad Kadhim[1], Naseer Hafedh Ibrahim[2]

[1] Al-Mansouriya Power Station, Ministry of Electricity, Diyala 32001, Iraq
[2] Department of College of Science, University of Diyala, Diyala 32001, Iraq

Corresponding Author Email: alighalib9567@gmail.com

https://doi.org/10.18280/rcma.360206

Received: 13 December 2025
Revised: 25 February 2026
Accepted: 9 March 2026
Available online: 30 April 2026

Keywords:
blast, sustainability, CO_2 emission, finite element method, ABAQUS

ABSTRACT

With the increasing exposure of civilian infrastructure to blast hazards, there is a critical need for protective systems that ensure structural performance, cost efficiency, and environmental sustainability. This study investigates the blast response and failure behavior of a composite wall system composed of adobe bricks and a recycled concrete aggregate (RCA) core arranged in a Brick–Recycled Aggregate–Brick (BRAB) configuration. Three-dimensional finite element simulations were conducted using ABAQUS/Explicit, with blast loading modeled through the ConWep formulation for a 1 kg Trinitrotoluene (TNT) charge at stand-off distances ranging from 0.25 m to 4.5 m. Two wall heights (4 m and 5 m) and three core thicknesses (30 cm, 60 cm, and 90 cm) were analyzed. Effects of reducing out-of-plane displacement in height to 36.5% and peak acceleration to seventy-seven% for 4 meter walls show that increasing core thickness greatly improves the blast resistance Walls with thick cores mainly correspond to Coulomb evaluation based on standard and Moconditioning to even at short stand-off distances, the proposed BRAB device achieves an additional 98% reduction in CO_2 emissions and a 95% saving in embodied energy and provides cost savings of up to 30% compared to conventional concrete walls. These findings highlight the potential of the BRAB wall as an effective, economical, and environmentally sustainable solution for blast mitigation in civilian infrastructure.

1. INTRODUCTION

Explosive risks from business injuries, terrorist attacks, and structural screw ups maintain to pose intense risks to civilian infrastructure globally, especially in city environments with excessive population densities. Blast masses generate intense shock waves that may set off intense dynamic responses in structures, leading to huge human casualties and considerable harm to buildings, utilities, and lifeline infrastructure. The layout of structural additives capable of mitigating blast consequences is therefore a crucial aspect of studies in structural engineering and protective design [1, 2].

High-composite-performance composite hybrid-metal concrete materials and engineered sandwich systems are commonly used in conventional blast mitigation responses, e.g., concrete composite panels with recycled rubber fibers under controlled blast forces have proven high-quality structural comparisons of blast [3]. Reducing dynamic variability and growth energy absorption of blast-loaded structures had answers in place [4]. However, the expensive, complex manufacturing strategy and huge environmental impact of modern materials and industrial techniques often keep them from their widespread acceptance. Current research in blast-resistant design also focuses on durability performance. Research has established that sustainable construction strategies and environmentally friendly composites can also provide appropriate structural performance by reducing the carbon footprint and embodied stress [5]. In a comparable vein, attempts were made to improve the blast resistance in concrete walls and masonry as developing [6]. Environmentally friendly materials and innovative structural design contribute to low-shore shield response without compromising safety standards. Despite these properties, studies on blast-resistant barriers may limit the use of field-on-hand, low-body strength materials, such as recycled concrete aggregate (RCA) and adobe bricks The present illustrations indicate a Brick–Recycled Aggregate–Brick (BRAB) brick-to-brick hatch wall material stacking of these high-stability 3-dimensional finite detail simulations completed in ABAQUS/Explicit, where blast pressures are simulated using the empirical ConWep version, BRAB walls under relaxed blast loads are tested for the structural smoothness performance of the Coulomb–Monn well potential as well structural failures are used to classify the environmental overall performance of the proposed device is classified in the assessment on conventional concrete partitions. This comprehensive strategy aims to highlight a way to approach sustainable and effective blast mitigation

strategies suitable for civilian infrastructure.

1.1 Literature review

A few years later, many studies on blast-resistant separations and boundaries generally found the basis for creating defense systems in response to the increasing risk of terrorist attacks on civilian infrastructure based on early research on the diffusion of knowledge, diffusion waves and their interaction. It focuses on improving system security.

1.1.1 Blast-resistant walls made of composites and multiple layers

The configuration and evaluation of multi-layer composite blast-resistant structures is now advanced. Recycled rubber fiber-impregnated blast-resistant concrete wall panels exhibited top-notch dynamic performance, achieving a high degree of safety under standardized blast mass and assembly design code requirements. These composite wall systems reduced structural deformation and blast deformation as demonstrated by the myth of crash.

Meanwhile, research on multi-use layered hybrid composite cleavage proved the importance of connection design and layer design to achieve high-quality blast response. Optimized composite walls can reduce peak deflection and postpone failure, as demonstrated by numerical modeling and experimental analysis [4]. The study of sustainable cracking and fracture mitigation strategies makes the case for combining structural safety goals with carbon management goals, especially in the design of low-carbon materials and safety systems [5].

1.1.2 Use of lightweight and energy-soft materials to prevent explosions

Surface treatments and coatings were investigated as secondary spray mitigation techniques. Protective coatings made of polyurea-polymer coatings can also prevent pressure wave propagation and reduce concrete floor fractures, attempting to reduce wall damage in the face of blast loads [6]. Systematic evaluation of wall response dynamics is feasible with experimental systems controlled by a few natural controls and in the laboratory, the effect of the threshold level [7].

1.1.3 The creation of the use of three sustainable recycled materials

Mechanical housing and the environmental benefits of green bricks, recycled castings and sustainable building materials have been explored. According to the study of recycled combination concrete, careful mix design and additional cementitious materials can produce tremendous mechanical performance, which indicates suitability for structural complexes where durability is top priority [8, 9] can achieve aggressive compressive strength and also reduce the cost of the high lightness, increasing the use of sustainable fabric concepts for blast-resistant wall systems [10].

Sustainable building products are becoming more popular with blast reduction. Environmental benefits and proper mechanical properties of RCA, demolition waste, and common masonry materials have been researched [9, 10]. Studies of masonry blocks for recycled construction particles show reduced embodied carbon and aggressive wood utilization potential [11]. Moreover, studies on alkali-activated mortars incorporating construction and demolition waste display promising sturdiness and mechanical performance [12]. These strains of research highlight possibilities to incorporate regionally sourced sustainable substances into blast-resistant wall structures.

1.1.4 Research gap and motivation

While large progress has been made in superior composite blast walls and sustainable creation substances, most present studies treat these subjects separately or specialize in static or seismic performance. Integrated critiques that connect cloth sustainability, blast overall performance, failure prediction, and value analysis are nevertheless constrained. The BRAB wall machine proposed in this take a look at ambitions to fill this gap by means of combining those aspects into a comprehensive framework to assess sustainable blast resistance for civilian infrastructure packages.

2. BLAST WAVE CHARACTERISTIC IN AIR

The wave resulting from the explosion has properties that change according to the type of explosive, the surrounding environment, how the wave interacts with the structure undergoing the explosion, and the extent of the change in the wave's structure. The wave structure is often the same for explosions in the free field (see Figure 1) [13].

Figure 1 shows the ideal time-related pressure profile for a free blast wave state. Due to high energy release, a rapid increase in atmospheric pressure is observed in a short time t_A to reach the pressure p_{s0}, and this is known as the peak pressure; then a rapid decrease in pressure occurs until it reaches the previous position at time $t_A + t_d$. The time from t_A to $t_A + t_d$ is known as the positive phase. After the positive phase of the compression time graph, the pressure becomes smaller (denoted as negative) than the ambient value and eventually returns to it. The negative phase starts from time $t_A + t_d$ to time $t_A + t_d + t_{d^-}$ [13, 14].

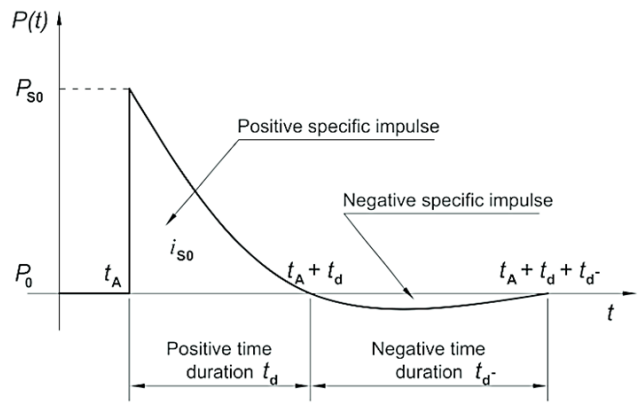

Figure 1. Idealized pressure–time history of a free-field blast wave showing positive and negative phases and peak overpressure

The negative phase is mainly ignored because it is much smaller than the positive phase and has little effect, but it does explain why there are pieces of glass outside the building instead of inside. Then the blast wave fades, and the air pressure returns to its normal state [15]. The blast wave in free air is described by Friedlander's equation, as shown in Eq. (1):

$$P(t) = P_{S0}\left[1 - \frac{t}{t_d}\right] e^{\left[\frac{-\alpha*(t-t_A)}{t_d}\right]} \quad (1)$$

where, $P(t)$ is the pressure at a certain time, P_{s0} is the highest pressure, t_d represents the time period of the positive phase, a is the damping factor in the wave, and t_A is the arrival period.

3. FINITE ELEMENT MODELING

The dimensions and geometry of the wall were proposed, where two different heights of the wall were used, and the thickness of the brick material was 15 cm. As for the thickness of the core, three different thicknesses were used. For the type of explosive used, it was proposed to use a charge of 1 kg of Trinitrotoluene (TNT) placed in the middle of the wall, as well as according to the different distances between the wall and the explosive charge, as shown in Figure 2.

3.1 Geometry definition

The BRAB wall geometry changed into described primarily based on two wall heights and 3 extraordinary middle thicknesses. Two wall heights of 4 m (W1) and 5 m (W2) were taken into consideration, at the same time as the wall width was kept consistent at 3 m. The wall consists of three layers organized in a BRAB configuration, wherein the front and back layers are adobe bricks with a constant thickness of 15 cm, and the middle layer consists of RCA with thicknesses of 30, 60, and 90 cm.

The geometric parameters of all wall configurations are summarized in Table 1, while a schematic representation of the wall geometry and explosive charge placement is shown in Figure 2. The different BRAB wall configurations for both wall heights are illustrated in Figure 3.

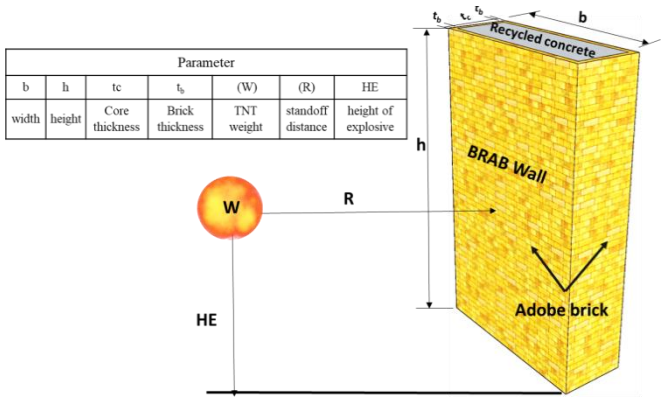

Figure 2. Schematic representation of the Brick–Recycled Aggregate–Brick (BRAB) wall geometry and Trinitrotoluene (TNT) explosive charge configuration used in the numerical model

Table 1. Geometry parameters of Brick–Recycled Aggregate–Brick (BRAB) wall

Model	Geometry Parameters			
	Height (h), m	Width (b), m	Core Thickness (t_c), cm	Adobe Brick Thickness (t_b), cm
W1	4	3	30, 60, 90	15
W2	5	3	30, 60, 90	

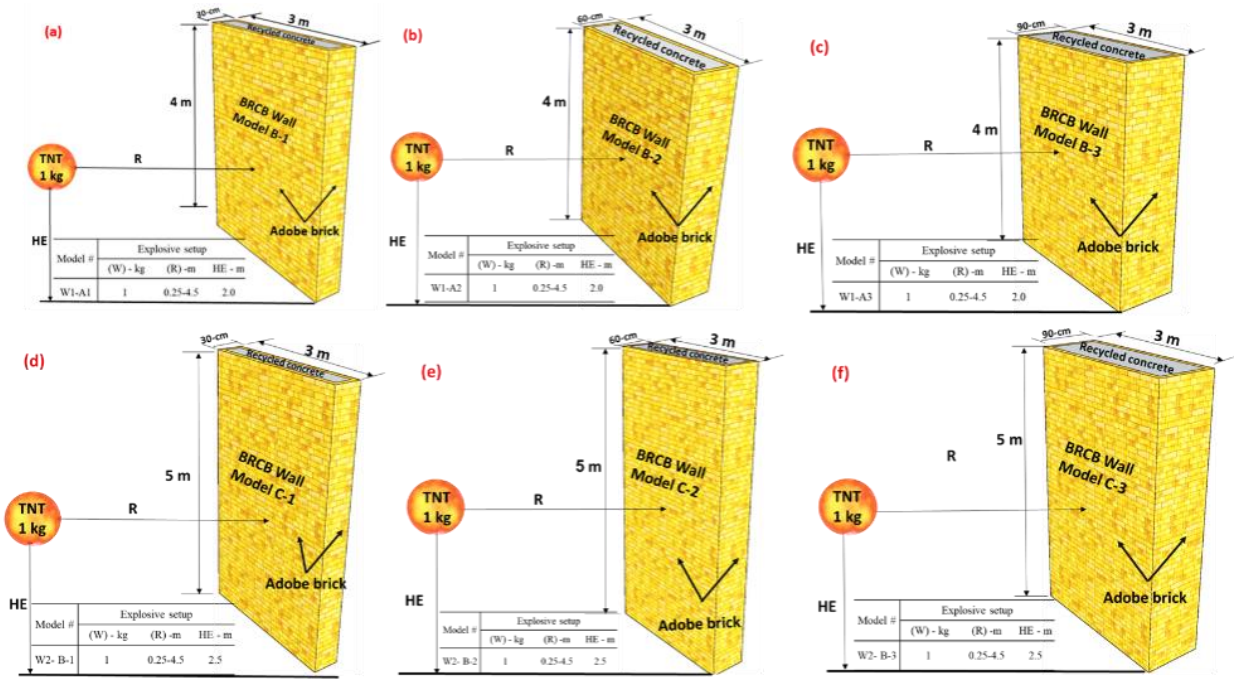

Figure 3. Configurations of the Brick–Recycled Aggregate–Brick (BRAB) wall system used in the numerical simulations: (a–c) wall type W1 with height = 4 m and recycled aggregate core thicknesses of 30 cm, 60 cm, and 90 cm; (d–f) wall type W2 with height = 5 m and recycled aggregate core thicknesses of 30 cm, 60 cm, and 90 cm

Note: Each wall consists of two external adobe brick layers (15 cm thickness each) surrounding a recycled concrete aggregate (RCA) core layer

3.2 Material properties

Two one-of-a-kind materials have been assigned to the wall components: adobe brick for the outside layers and recycled concrete mixture for the core layer. The mechanical properties of adobe bricks, including density, Young's modulus, and Poisson's ratio, were adopted from experimental research pronounced inside the literature and are listed in Table 2. The

recycled mixture middle was modeled using fabric homes derived from sieve evaluation and previous research, as supplied in Table 3.

Both substances had been assumed to behave as linear elastic isotropic substances. This assumption is justified via the short period of blast loading and the goal of the study, which specializes in worldwide wall response and failure prediction based on stress limits in preference to distinctive crack propagation. Similar assumptions have been broadly adopted in preliminary numerical investigations of blast-resistant structures.

As for the mechanical properties of the RCA, the results obtained from the sieve analysis.

Table 2. Characteristics of the adobe brick material

Density (kg/m^3)	1300
Poisson's ratio	0.35
Young's modulus (MPa)	135

Table 3. Characteristics of the recycled aggregate

Density (kg/m^3)	1395
Poisson's ratio	0.25
Young's modulus (MPa)	10

3.3 Element type and mesh details

The BRAB wall became discretized using 3-dimensional eight-node linear brick elements with decreased integration (C3D8R), which are appropriate for dynamic explicit evaluation and green computation of brief-period blast occasions. A dependent mesh was used for all wall configurations to ensure numerical stability and accuracy.

A mesh sensitivity takes a look at changed into carried out to ensure that the numerical results are not considerably suffering from mesh length. Based on this have a look at, a median element size of approximately one hundred mm was selected as a compromise between computational efficiency and solution accuracy. The very last finite detail mesh of the BRAB wall version is proven in Figure 4.

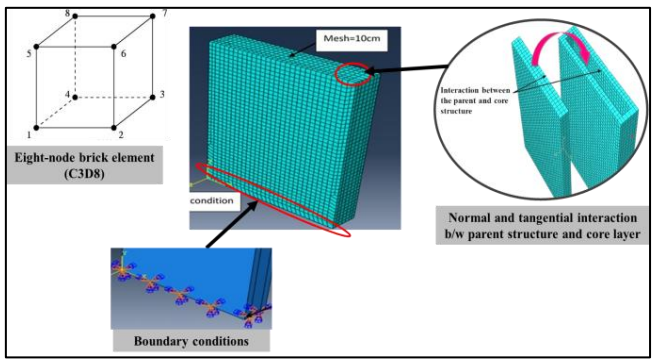

Figure 4. Three-dimensional finite element mesh of the BRAB wall model developed in ABAQUS/Explicit using C3D8R elements

3.4 Boundary conditions

The wall became assumed to be rigidly connected to the floor. Accordingly, all translational and rotational tiers of freedom at the bottom of the wall have been fully confined, representing a set assist circumstance. This boundary circumstance simulates practical setup situations in which blast walls are anchored to inflexible foundations.

3.5 Interaction definition

The interaction between the adobe brick layers and the recycled aggregate middle is modeled using a floor-to-surface touch formula. A friction coefficient of 0.4 turned into assigned between the contacting surfaces to simulate the interaction conduct between beaten concrete aggregates and adobe bricks. Partial overlap between the layers becomes defined to make sure right load transfer throughout blast loading, as illustrated in Figure 3(c).

3.6 Blast load application

Blast loading was carried out the usage of the ConWep blast version available in the ABAQUS load library. The Conventional Weapons Effects Program (ConWep) model is primarily based on the empirical Kingery–Bulmash equations and is extensively used to simulate unconfined-discipline blast wave–shape interaction. A TNT equivalent charge weight of 1 kg was adopted for all analyses.

The explosive price becomes positioned at the centerline of the wall at diverse standoff distances starting from 0.5 m to 4.0 m, as proven in Figure 2. The blast pressure–time history was mechanically generated by the ConWep version based on the desired rate, weight and standoff distance. Dynamic express analysis was completed with a total simulation time of zero.3 s, which became sufficient to capture the complete blast reaction of the wall [16].

The numerical simulations were performed using the dynamic explicit analysis module of ABAQUS/Explicit (version 6.14) [17]. The explicit solver was adopted to efficiently capture the highly dynamic and nonlinear response of the structure under short-duration blast loading.

Blast loading was applied using the ConWep model, which is based on the Kingery–Bulmash empirical equations [18, 19]. The model requires the explosive charge weight and location as input parameters and was used to simulate free-field blast wave interaction. A TNT equivalent charge of 1 kg was considered, and the standoff distance was varied from 0.5 m to 4.0 m.

The total analysis time was set to 0.3 s, which was sufficient to capture the complete structural response of the BRAB wall under blast loading.

4. THE PROPERTIES OF AGGREGATE OF CRUSHED CONCRETE

A blast-resistant wall system is proposed that can be constructed using simple techniques, with low construction cost and minimal requirement for skilled labor. Sustainable materials that are abundantly available and inexpensive were used in the construction of the proposed wall system. Where the wall consists of two main parts, which are the container and the core. As for the container part, it consists of the Adobe Brick material. As for the core area, it consists of the existing crushed RCA (Figure 5). The sieve analysis of the RCA was carried out according to ASTM C33, as shown in Figure 5. And through the sieve analysis, the fineness coefficient of the RCA was found, which is 2.7 [20].

As for the mechanical properties of the adobe bricks, as

shown in Table 2 [21]. As for the compressive strength of the bricks, it was equal to 1.03 MPa, and the tensile strength was equal to 0.22 MPa [22].

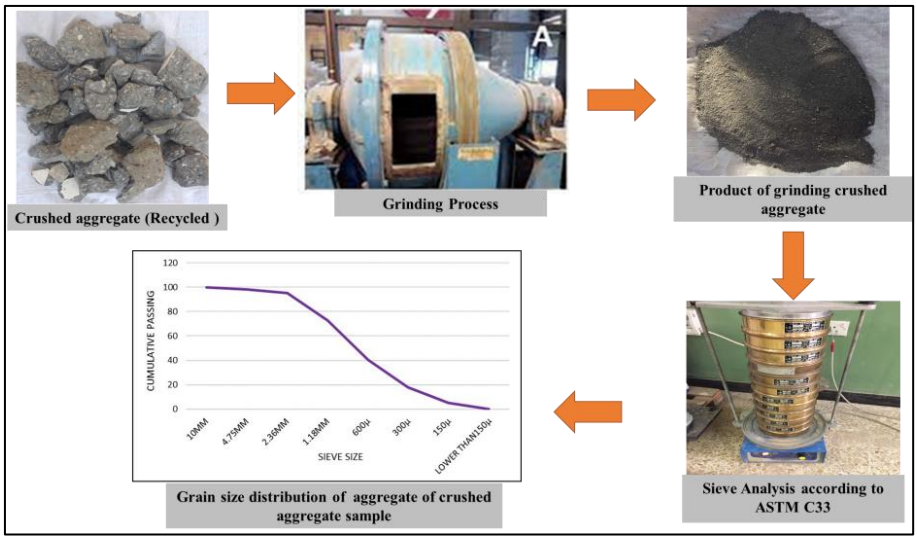

Figure 5. Particle size distribution of recycled concrete aggregate (RCA) obtained from sieve analysis according to ASTM C33 standards

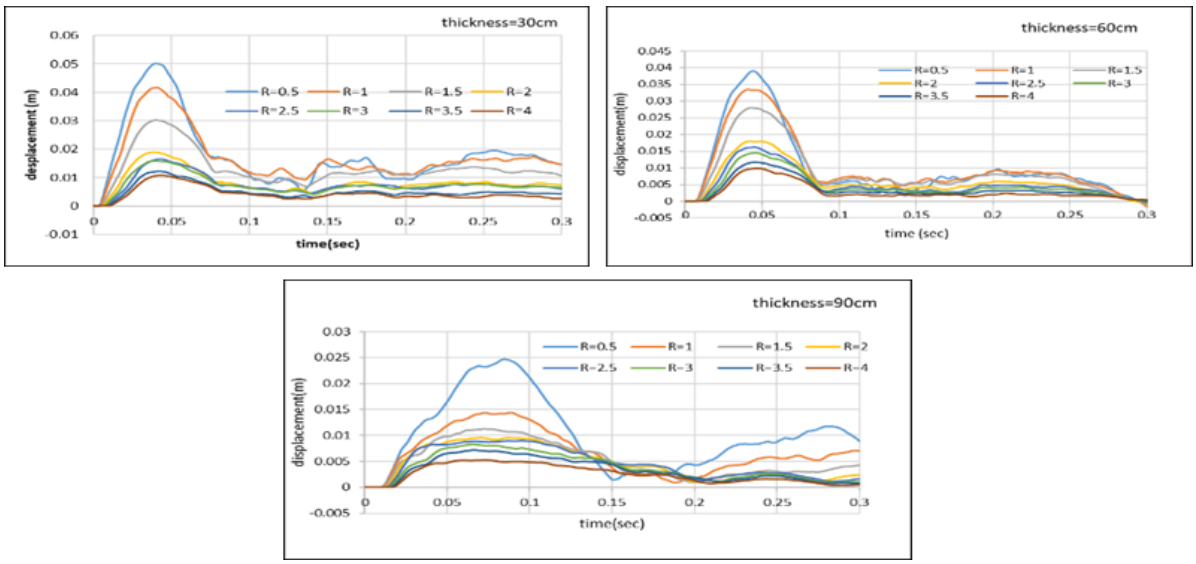

Figure 6. Time-history response of out-of-plane displacement for BRAB wall (W1, height = 4 m) under 1 kg TNT blast at varying stand-off distances and core thicknesses
Note: BRAB = Brick–Recycled Aggregate–Brick, TNT = Trinitrotoluene

5. NUMERICAL ANALYSIS RESULTS OF BRICK–RECYCLED AGGREGATE–BRICK WALL

Analytical results using Abaqus software showed displacements in walls of different thicknesses in addition to the acceleration.

Figure 6 presents the time-history response and time of the displacement in the BRAB blast wall W1 due to the explosion spectrum and response from the standoff distance of three different thicknesses, 30, 60, and 90 cm, respectively. In general, the displacement decreases as the standoff distance increases if the explosive charge is stationary and when the thickness of the core layer increases. For example, at a distance of 0.5 m, the peak displacement is 0.0503 m. while it decreases to 0.0435 m when the standoff distance increases to 1 m. Moreover, the displacement reduction is 22.4% when the wall thickness is increased to 60 cm and is 51.3% when the core thickness is 90 cm. The displacement peak is shown in Table 4.

Table 4. Numerical results of peak displacement of Brick–Recycled Aggregate–Brick **(**BRAB**)** wall W1

Distance (m)	t_c = 30 cm (m)	t_c = 60 cm (m)	t_c = 90 cm (m)
0.5	0.0503	0.0388	0.0245
1.0	0.0435	0.0340	0.0143
1.5	0.0319	0.0275	0.0117
2.0	0.0188	0.0172	0.0099
2.5	0.0166	0.0160	0.0087
3.0	0.0156	0.0144	0.0083
3.5	0.0125	0.0113	0.0071
4.0	0.0109	0.0097	0.0052

The acceleration time-history response of the BRAB W1 blast wall is estimated with three different thicknesses of 30, 60, and 90 cm, respectively. The calculated peak acceleration is 3212.03 m/sec² when 1 kg of TNT is placed 0.5 m from the wall, while it decreases to 1842.1 m/sec² when the explosive charge is detonated at 1 m. However, a decreased response was observed when the charge was placed 4 m in front of the wall. Table 5 and Figure 7 show the peak acceleration of the BRAB blast wall W1 in terms of standoff distance with three different core thicknesses [23].

Figure 8 presents the time-history response and time of displacement of the BRAB W2 blast wall due to the blast spectrum and response from a standoff distance of three different thicknesses, 30, 60, and 90 cm, respectively. In general, the displacement decreases as the standoff distance increases if the explosive charge is stationary and when the thickness of the core layer increases [24]. For example, at a distance of 0.5 m, the peak displacement is 0.0422, while it decreases to 0.0382 m when the standoff distance increases to 1 m. Moreover, the displacement reduction is 14% when the wall thickness is increased to 60 cm, and is 52.36% when the core thickness is 90 cm. The displacement peak is shown in Table 6.

Table 5. Numerical results of peak acceleration of Brick–Recycled Aggregate–Brick (BRAB) wall W1

Distance (m)	Acceleration (m/sec²)		
	t_c = 30 cm	t_c = 60 cm	t_c = 90 cm
0.5	3212.03	2563.28	737.088
1.0	1842.1	1324.08	325.965
1.5	888.064	556.838	235.332
2.0	528.674	375.273	180.303
2.5	455.886	249.004	106.646
3.0	103.303	80.9765	45.8791
3.5	87.1035	68.375	39.895
4.0	50.0258	43.3845	30.6117

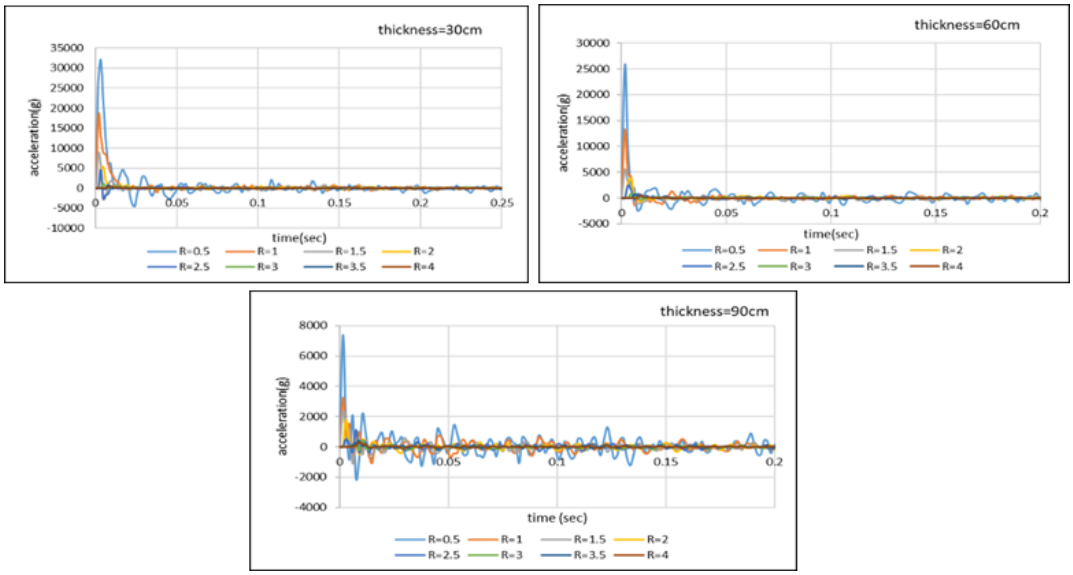

Figure 7. Time-history response of out-of-plane displacement for BRAB wall (W2, height = 5 m) under 1 kg TNT blast at varying stand-off distances and core thicknesses
Note: BRAB = Brick–Recycled Aggregate–Brick, TNT = Trinitrotoluene

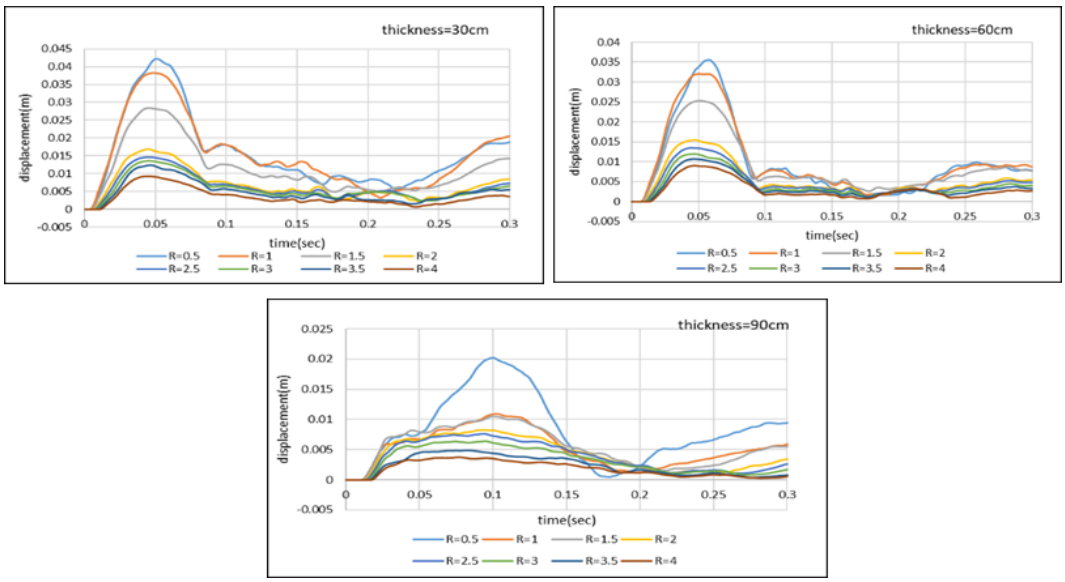

Figure 8. Peak acceleration response of BRAB wall (W1) for different recycled aggregate core thicknesses under blast loading
Note: BRAB = Brick–Recycled Aggregate–Brick

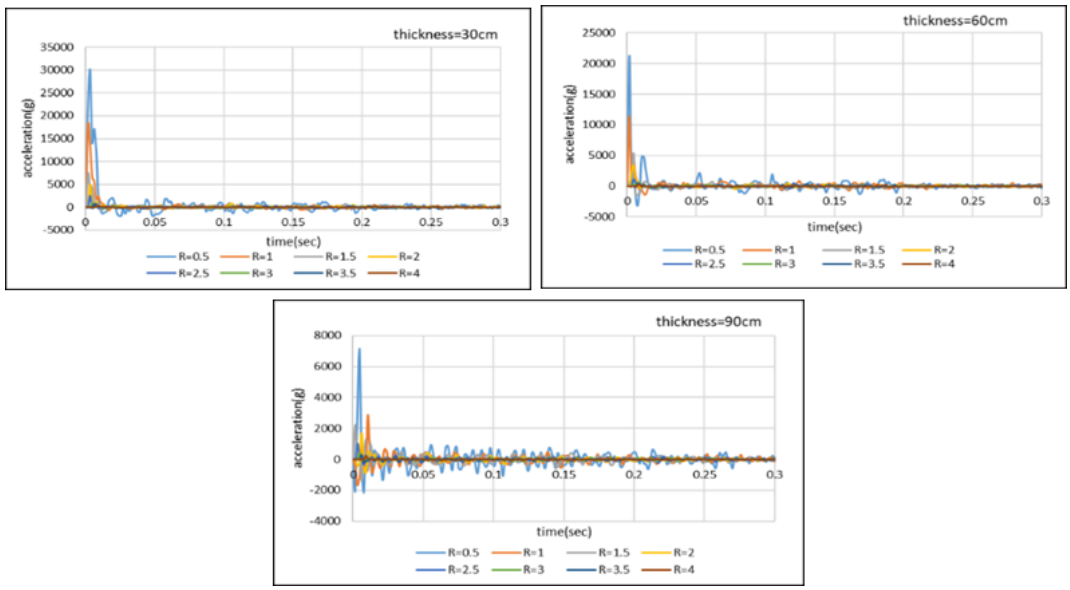

Figure 9. Peak acceleration response of BRAB wall (W2) for different recycled aggregate core thicknesses under blast loading
Note: BRAB = Brick–Recycled Aggregate–Brick

In Figure 9, the acceleration history of the BRAB W2 wall is shown in three different thicknesses of 30, 60, and 90 cm, respectively. The calculated peak acceleration is 3002.24 m/sec² when 1 kg of TNT is placed at a distance of 0.5 m from the wall, while it decreases to 1781.04 m/sec² when the explosive charge is detonated at 1 m. However, a reduced response was observed when the charge was placed 4 m in front of the wall. Table 7 shows the peak acceleration of the BRAB blast wall W3 in terms of the distance between the wall and the blast charge for three different base thicknesses.

Table 6. Numerical results of peak displacement of Brick–Recycled Aggregate–Brick **(**BRAB**)** wall W2

R	Displacement (m)		
	t_c = 30cm	t_c = 60 cm	t_c = 90 cm
0.5	0.04224	0.0363	0.0201
1	0.03823	0.0324	0.0112
1.5	0.02761	0.0251	0.0100
2	0.01678	0.0154	0.0082
2.5	0.01498	0.0134	0.0077
3	0.01360	0.0118	0.0063
3.5	0.01206	0.0107	0.0048
4	0.00906	0.0088	0.0034

Table 7. Numerical results of peak acceleration of Brick–Recycled Aggregate–Brick **(**BRAB**)** wall W2

R	Peak Acceleration (m/sec2)		
	t_c = 30 cm	t_c = 60 cm	t_c = 90 cm
0.5	3002.24	2127.91	708.489
1	1781.04	1144.06	287.819
1.5	744.521	535.437	221.977
2	497.746	340.406	166.405
2.5	257.912	114.335	101.176
3	96.1299	51.3133	41.1359
3.5	77.84	38.2133	27.3121
4	39.4514	23.4283	21.0931

6. FAILURE PREDICTION OF BRAB BLAST WALL

The Coulomb-Mohr failure criterion is a mathematical model used to illustrate and predict the failure of brittle materials. It is used in structural engineering in order to determine the failure that occurs in brittle materials upon increased load. This theory has the distinction of being one of the most common failure criteria for brittle materials, being more computationally simple and accurate [25]. The criterion considered a set of linear equations between maximum and minimum principal stresses (normal and shear stresses) at failure. The Coulomb-Mohr failure criterion uses Mohr circles to construct a failure envelope [25].

The Coulomb-Mohr envelope shows two circles that represent compression stress as well as tensile stress, and two tangential lines to the two circles. If the generated stress magnitude is outside of the two lines, this indicates material failure, while the safe zone is in between the two lines. The mathematical equation depends on both σ1 and σ3, as shown in Eq. (2) [26].

$$\frac{\sigma 1}{\sigma t} - \frac{\sigma 2}{\sigma c} = 1 \qquad (2)$$

where,

- $\sigma 1$ = maximum principal stress
- $\sigma 2$ = minimum principal stress
- σt = uniaxial tensile strength
- σc = uniaxial compressive strength

In this thesis, the Coulomb-Mohr criterion is used to determine failure in the adobe brick when subjected to blast load, which represents the failure threshold of the BRAB blast wall.

The current study considered the Coulomb-Mohr failure criterion to predict the failure of the BRAB wall. The results of the interaction equation indicate whether the wall fails or not based on the induced stress due to the blast load. The stress (σ1 and σ3) values were found from the program for distances per quarter meter (0.25 m to 4.5 m) for all walls and were compensated within the previously mentioned failure equation to determine whether the wall fails when placing the charge at a certain distance.

Figure 10 shows the failure index of the BRAB blast wall W1. When the core thickness of the wall is 30 cm, the wall failed when placing the explosive charge at a distance less than

3.75 m. When the core thickness of the wall is increased to 60 cm, the wall failed when placing the charge at a distance less than 3 m. When the core thickness was increased to 90 cm, the wall failed when placing the charge at a distance less than 1 m.

Figure 11 illustrates the failure index of the BRAB blast wall W2. When the core thickness was 30 cm, the wall failed when placing the charge at a distance less than 3.25 m. However, the wall with a 60 cm core thickness failed when placing the charge at a distance less than 2.75 m. The wall with a 90 cm thickness failed when the distance between the explosive charge and the wall was less than 0.25 m.

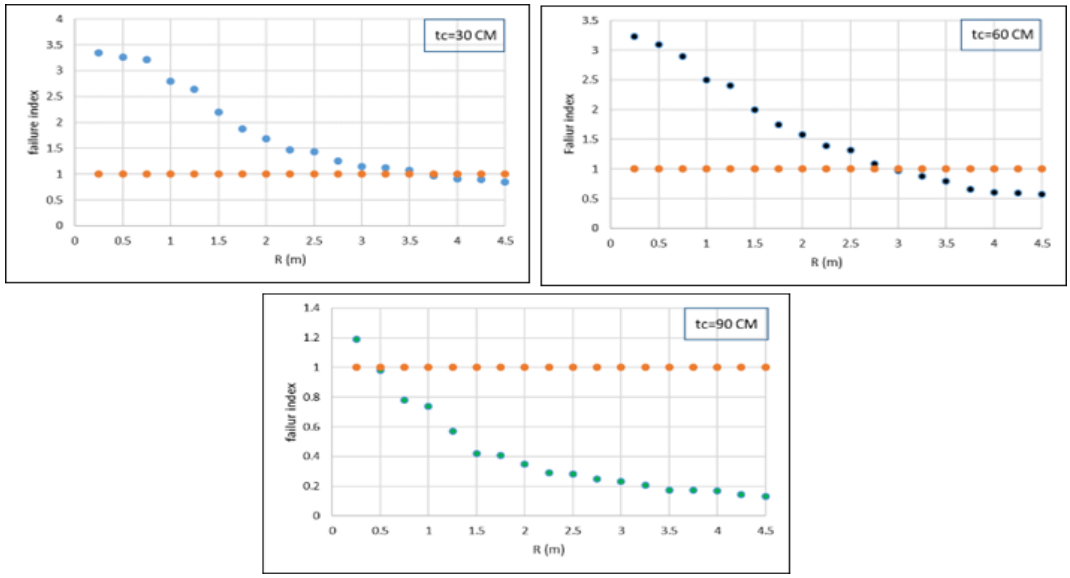

Figure 10. Maximum principal stress distribution in BRAB wall subjected to blast loading for failure evaluation using the Coulomb–Mohr criterion
Note: BRAB = Brick–Recycled Aggregate–Brick

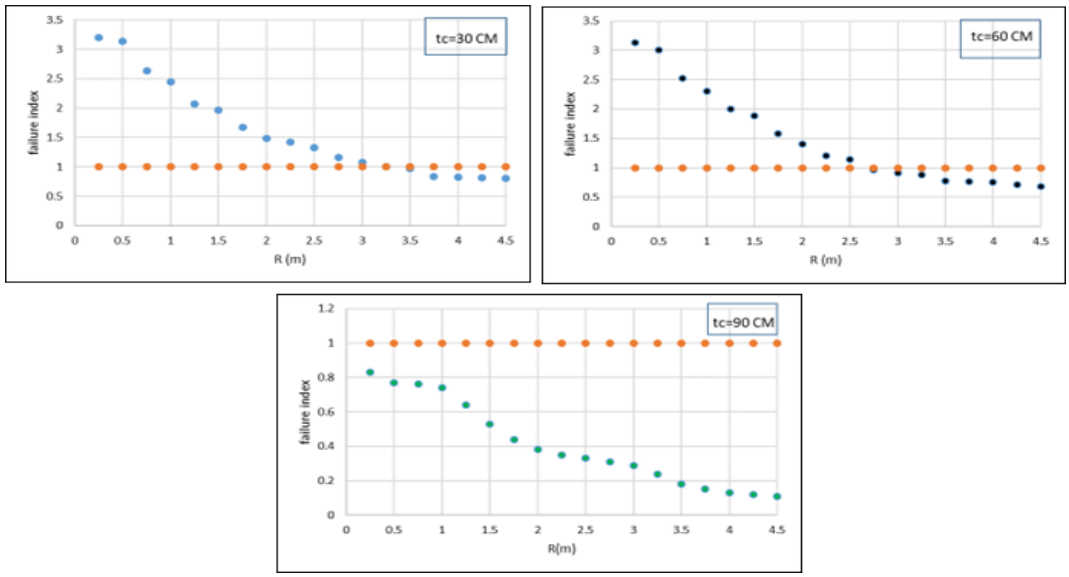

Figure 11. Comparison of failure modes of BRAB wall configurations based on the Coulomb–Mohr failure criterion under different stand-off distances
Note: BRAB = Brick–Recycled Aggregate–Brick

7. COST SAVING OF THE BRAB WALLS

Recycled aggregates and mud bricks were used in the blast wall modeling process. The use of bricks is one way to make construction environmentally friendly, inexpensive, and easy to manufacture, and the use of recycled concrete reduces the consumption of natural materials such as sand and gravel. The cost of the BRAB wall was calculated by assuming that the wall is built in the form of a single block by using one mold for the wall, and it was compared to the cost of building an unreinforced concrete wall according to the mixing ratios (4:2:1).

7.1 Cost saving of the Brick–Recycled Aggregate–Brick wall W1

Table 8 shows the effect of using sustainable materials on the cost of constructing BRAB Wall W1. Note that the cost of the wall thickness of BRAB 30 cm, BRAB 60 cm, and BRAB 90 cm decreased by 30%, 19.6%, and 14.7%, respectively.

7.2 Cost saving of the Brick–Recycled Aggregate–Brick wall W2

Table 9 shows the effect of using sustainable materials on the cost of constructing a BRAB Wall W2. Note that the cost of the wall thickness of BRAB 30 cm, BRAB 60 cm, and BRAB 90 cm decreased 30%, 20%, and 14.7%, respectively.

Table 8. Cost calculations of Brick–Recycled Aggregate–Brick (BRAB) wall (W1) compared to a concrete wall (CW)

Model W1	Volume (m^3)					Weight (tons)					Price Iraqi Dinar	
	Adobe	Recycled Concrete	Sand	Gravel	Cement	Adobe	Recycled Concrete	Sand	Gravel	Cement	Total
BRAB 30 cm	4.1	3.1	---	---	---	78000	216000	---	---	---	294000
BRAB 60 cm	4.6	6.23	---	---	---	86000	435500	---	---	---	521500
BRAB 90 cm	5.05	9.35	---	---	---	96000	650000	---	---	---	746000
CW 60 cm	---	---	3.1	6.3	2.1	---	---	70000	120000	227000	417000
CW 90 cm	---	---	4.8	9.5	3.2	---	---	110000	180000	350000	640000
CW 120 cm	---	---	6.4	12.7	4.3	---	---	145000	240000	470000	855000

Table 9. Cost calculations of Brick–Recycled Aggregate–Brick (BRAB) wall (W2) compared to a concrete wall (CW)

Model W2	Volume (m^3)					Weight (tons)					Price Iraqi Dinar	
	Adobe	Recycled Concrete	Sand	Gravel	Cement	Adobe	Recycled Concrete	Sand	Gravel	Cement	Total
BRAB 30 cm	5.1	3.9	---	---	---	97000	270000	---	---	---	367000
BRAB 60 cm	5.7	7.85				108000	550000	---	---	---	658000
BRAB 90 cm	6.2	11.8	---	---	---	118000	825000	---	---	---	943000
CW 60 cm	---	---	4	8	2.7	---	---	90000	150000	291000	531000
CW 90 cm	---	---	6	12	4.2	---	---	135000	225000	455000	815000
CW 120 cm	---	---	8	16	5.4	---	---	180000	300000	585000	1065000

8. SUSTAINABILITY BENEFITS OF THE BRICK–RECYCLED AGGREGATE–BRICK WALLS

Adobe bricks and recycled concrete are sustainable materials that have less of an impact on the environment, as the carbon dioxide emissions from their manufacture are very low. For the purpose of knowing the environmental impacts of the BRAB wall and comparing it with the concrete neighbor. Embodied energy and CO_2 emissions were calculated when the adobe brick was manufactured [25]. As for the crushing of concrete residues, it is done by knowing the amount of energy used and the emission of carbon dioxide from the grinding machine (see Table 10).

As for the embodied energy, as well as the emission of carbon dioxide to produce the concrete wall, it is represented by calculating the environmental impact of each of sand, gravel, and cement (see Table 11) [27].

8.1 Sustainability benefits of the Brick–Recycled Aggregate–Brick wall W1

For the BRAB 30 cm, 60 cm, and 90 cm walls, Tables 12 and 13 show a reduction of approximately 98.8%, 98.7%, and 98.65% in CO_2 emissions, and about 95.9%, 95.5%, and 95.27% in embodied energy, respectively.

8.2 Sustainability benefits of the Brick–Recycled Aggregate–Brick wall W2

Tables 14 and 15 show the reductions in CO_2 emissions and embodied energy for walls BRAB 30 cm, BRAB 60 cm, and BRAB 90 cm, at 98.8%, 98.76%, and 98.65%, respectively. The embodied energy decreased by 96%, 95.6%, and 95.3%.

Table 10. CO_2 emissions and combined energy of Brick–Recycled Aggregate–Brick (BRAB) wall component

	Adobe Brick	Recycle Concrete
Embedded energy (MJ/kg)	0.033	0.088
CO_2 emission (kg/kg)	0.0017	0.0037

Table 11. CO_2 emission and embedded energy of concrete wall component [26]

	Sand	Gravel	Cement
Embedded energy (MJ/kg)	0.1	0.04	6.2
CO_2 emission (kg/kg)	0.007	0.002	0.994

Table 12. CO_2 emission and embedded energy of Brick–Recycled Aggregate–Brick (BRAB) wall W1

Model	BRAB 30 cm			BRAB 60 cm			BRAB 90 cm		
	Weight (kg)	Embodied Energy (MJ)	CO_2 (kg)	Weight (kg)	Embodied Energy (MJ)	CO_2 (kg)	Weight (kg)	Embodied Energy (MJ)	CO_2 (kg)
Adobe	5330	179.5	9.06	5859	193.05	10	6565	216.6	11.16
Recycled Concrete	4324	380.5	16	8690	775.8	32.15	13043	1147.8	48.25
Total		560	25.06		968.85	42.15		1364.4	59.41

Table 13. CO_2 emission and embedded energy of concrete wall (CW) W1

Model	CW 60 cm			CW 90 cm			CW 120 cm		
	W (kg)	Embodied Energy (MJ)	CO_2 (kg)	W (kg)	Embodied Energy (MJ)	CO_2 (kg)	W (kg)	Embodied Energy (MJ)	CO_2 (kg)
Sand	5600	560	39.2	8400	840	58.8	11200	1120	78.4
Gravel	12800	512	25.6	19200	768	38.4	25600	1024	51.2
Cement	2700	16740	2638.8	4200	26040	4174.8	5400	33480	5367.6
Total		17812	2703.6		27648	4272		35624	5497.2

Table 14. CO_2 emission and embedded energy of Brick–Recycled Aggregate–Brick **(**BRAB**)** wall W2

Model	BRAB 30 cm			BRAB 60 cm			BRAB 90 cm		
	Weight (kg)	Embodied Energy (MJ)	CO_2 (kg)	Weight (kg)	Embodied Energy (MJ)	CO_2 (kg)	Weight (kg)	Embodied Energy (MJ)	CO_2 (kg)
Adobe	6630	218.79	11.27	7410	244.5	12.6	8060	265.98	13.702
Recycled Concrete	5440.5	478.7	20.12	10950.7	963.66	40.5	16461	1448.5	60.9
Total		697.5	31.39		1208.16	52.9		1714.48	74.6

Table 15. CO_2 emission and embedded energy of concrete wall (CW) W2

Model	CW 60 cm			CW 90 cm			CW 120 cm		
	Weight (kg)	Embodied Energy (MJ)	CO_2 (kg)	Weight (kg)	Embodied Energy (MJ)	CO_2 (kg)	Weight (kg)	Embodied Energy (MJ)	CO_2 (kg)
Sand	4340	434	30.38	6720	672	47.04	8960	896	62.7
Gravel	10080	403	20.16	15200	608	30.4	20320	812.8	40.6
Cement	2100	13020	2087	3200	19840	3180.8	4300	26660	4274.2
Total		13857	2137.54		21120	3258.24		28368	4377.5

9. DISCUSSION

The numerical consequences reveal that the blast response of the BRAB wall is strongly governed by the thickness of the recycled aggregate core and, to a lesser extent, by the wall peak. Unlike conventional monolithic concrete walls, the BRAB system behaves as a layered composite wherein the granular middle performs a dominant position in attenuating blast-prompted stress waves.

The amount of interconnected elements may be responsible for a certain reduction in acceleration and peak displacement with better core thickness. The recycled mixture core first releases electricity through interparticle friction and particle rearrangement, which converts kinetic energy into local distortion and heat and is a mistake strategy that provides a mixture of imp on why there is a disproportionately large acceleration reaction reduction when the thickness of the center improves from 30 cm to ninety cm. The protective role of the connection center is likewise proven through the failure prediction effect based on the Coulomb-Mohr criteria. Walls can withstand blast mass beyond fabric-strength limitations due to the fact that it postpones the occurrence of tensile stress concentrations within adobe brick tensile crack control, a tensile failure.

BRAB walls have more deformation rates than blast-resistant strategies encouraged in the literature, including metal reinforced concrete partitions or engineered sandwich panels, but it accomplishes this performance in a way with lower fabric load and environmental impact. This case study demonstrates that BRAB tools are operational when top is top performing for efficiency, economic feasibility and moderate blast resistance. It should be noted that the present Figs use the ConWep technique for simplified loose stiffness burst loads and linear elastic material failure. These estimates may underestimate local loss and confirm under-yield behavior, although they are suitable for preliminary assessment and comparative assessment. Further studies should include nonlinear fabric fashions, sophisticated scattering-structure interaction strategies, and experimental validation to further strengthen the design in question.

10. CONCLUSIONS

Focused on prediction of failure, structural response, cost performance, and environmental impact, this experiment provided a numerical evaluation of brick-reinforced mixed composite walls under blast flow. Effects of wall top, core thickness, and standoff distance were carefully evaluated using 3-dimensional ultimate element simulation.

Results show that increasing the thickness of the recirculation mixer improves the overall performance of crack reduction, especially by reducing peak displacement, acceleration, and failure rate. Thick cores allow walls to encounter closer crack distances when they move out past the electric field. Increased performance per stage, wall devices significantly reduce CO_2 emissions, embodied energy and construction costs compared to conventional concrete walls.

The primary contribution of this work lies in demonstrating that effective blast mitigation may be executed using locally available, recycled, and low-electricity materials without reliance on advanced composites or steel reinforcement. While the prevailing findings are based on numerical simulations, they provide a strong basis for future experimental research

and the development of practical layout pointers for sustainable blast-resistant infrastructure.

REFERENCES

[1] Shadan, P., Sharafi, P., Saeed, N. (2024). Blast response and protection level of concrete composite wall panels made with recycled tyre fibres in a cement matrix. Construction and Building Materials, 451: 138866. https://doi.org/10.1016/j.conbuildmat.2024.138866

[2] Laycock, A., Helliker, A., Critchley, R., Hazael, R. (2025). Transitioning to low carbon construction: A review of blast and fragmentation impact research related to terrorist threats. Structures, 78: 109173. https://doi.org/10.1016/j.istruc.2025.109173

[3] Park, Y., Kim, K., Park, S.W., Yum, S.G., Baek, J.W. (2024). Experimental evaluation on blast resistance of reinforced concrete structures under partially confined explosion. International Journal of Concrete Structures and Materials, 18: 34. https://doi.org/10.1186/s40069-024-00663-2

[4] Ahmad, S., Zeb, S., Wang, Y., Umair, M. (2025). Blast performance of multi-layer composite door panel with energy absorption connectors. Buildings, 15(12): 2073. https://doi.org/10.3390/buildings15122073

[5] Hamza, F., AliBoucetta, T., Behim, M., Bellara, S., Senouci, A., Maherzi, W. (2025). Sustainable self-compacting concrete with recycled aggregates, ground granulated blast slag, and limestone filler: A technical and environmental assessment. Sustainability, 17(8): 3395. https://doi.org/10.3390/su17083395

[6] Morsel, A., Masi, F., Marché, E., Racineux, G., Kotronis, P., Stefanou, I. (2024). miniBLAST: A novel experimental setup for laboratory testing of structures under blast loads. Experimental Techniques, 49: 655-675. https://doi.org/10.1007/s40799-024-00771-4

[7] Eissa, M., Habib, A., Al Houri, A., Alibrahim, B. (2024). Recent efforts on investigating the effects of recycled rubber content on the mechanical properties of structural concrete. Discover Civil Engineering, 1: 16. https://doi.org/10.1007/s44290-024-00017-7

[8] Mohamed, O.A., Ghanam, O., Hamdan, A., Zuaiter, M., Kim, T.Y. (2025). Mechanical properties and durability of concrete with recycled air-cooled blast furnace slag aggregates. Scientific Reports, 15: 24384. https://doi.org/10.1038/s41598-025-09242-1

[9] Parra, C., Miñano, I., Calabuig, M., Benito, F., Mateo, J. M., Carrión, E., Ruiz, C. (2024). Geopolymer with brick and concrete demolition construction waste. Materiales de Construcción, 74(356): e361. https://doi.org/10.3989/mc.2024.392424

[10] Çavuş, M., Kaplan, G., Aruntaş, H.Y., Dayı, M. (2025). Sustainable lightweight wall blocks from recycled construction waste: The role of diatomite in mechanical ecological and thermal optimization. Construction and Building Materials, 473: 140993. https://doi.org/10.1016/j.conbuildmat.2025.140993

[11] Al-Naghi, A.A.A., Ali, T., Inam, I., Qureshi, M.Z., Ben Kahla, N., Ghazouani, N. (2025). An innovative approach to enhancing the strength and durability of recycled aggregate concrete through fly ash-silica fume coating and rice husk ash supplementation. Scientific Reports, 15: 32780. https://doi.org/10.1038/s41598-025-18138-z

[12] Güzelküçük, S., Şahin, O., Eren, Ş., Ulugöl, H. (2025). Alkali-activated mortars incorporating construction and demolition waste and industrial by-products: A fresh and hardened state evaluation. Gazi University Journal of Science, 38(4): 1742-1752. https://doi.org/10.35378/gujs.1637907

[13] Ngo, T.D., Mendis, P.A., Gupta, A., Ramsay, J. (2007). Blast loading and blast effects on structures – An overview. Electronic Journal of Structural Engineering, (1): 76-91. https://doi.org/10.56748/ejse.671

[14] Cullis, I.G. (2001). Blast waves and how they interact with structures. Journal of the Royal Army Medical Corps, 147(1): 16-26. https://doi.org/10.1136/jramc-147-01-02

[15] Sochet, I., Schneider, H. (2010). Blast wave characteristics and equivalency. In Explosion Dynamics and Hazards, pp. 169-184. https://hal.science/hal-00606092v1.

[16] Wang, G.H., Wang, Y.X., Lu, W.B., Zhou, W., Chen, M., Yan, P. (2020). On the determination of mesh size for numerical simulations of shock wave propagation in near-field underwater explosion. Applied Ocean Research, 59: 1-9. https://doi.org/10.1016/j.apor.2016.05.011

[17] Kuang, Z.P., Liu, Z.H. (2023). Study on the mesh size determination method of blast wave numerical simulation with strong applicability. Heliyon, 9(2): e13714. https://doi.org/10.1016/j.heliyon.2023.e13714

[18] Kingery, C.N., Coulter, G.A. (1983). Reflected overpressure impulse on a finite structure. Final Report Ballistic Research Labs., Aberdeen Proving Ground, MD.

[19] Abaqus. (2016). Deformation of a sandwich plate under CONWEP blast loading. In Abaqus Example Problems Guide. Dassault Systèmes Simulia Corp., Providence, RI, USA. http://130.149.89.49:2080/v2016/books/exa/ch09s01aex138.html.

[20] Si, D.D., Pan, Z.F., Zhang, H.P. (2023). Determination of mesh size for numerical simulation of blast load in near-ground detonation. Defence Technology, 38: 111-125. https://doi.org/10.1016/j.dt.2023.08.004

[21] Salih, M.M., Osofero, A.I., Imbabi, M.S. (2020). Critical review of recent development in fiber reinforced adobe bricks for sustainable construction. Frontiers of Structural and Civil Engineering, 14: 839-854. https://doi.org/10.1007/s11709-020-0630-7

[22] Illampas, R., Ioannou, I., Charmpis, D.C. (2011). A study of the mechanical behaviour of adobe masonry. WIT Transactions on The Built Environment, 118(12): 485-496. https://doi.org/10.2495/STR110401

[23] Qader, Z.B., Karabash, Z., Cabalar, A.F. (2023). Analyzing geotechnical characteristics of soils in erbil via gis and artificial neural networks. Sustainability, 15(5): 4030. https://doi.org/10.3390/su15054030

[24] Salah, L.I., Al Douri, A.A., Khudher, M.E. (2025). Evaluating the geotechnical properties of the soil of the Sport City, West of Tikrit. Iraqi National Journal of Earth Science (INJES), 25(4): 65-77. https://doi.org/10.33899/earth.2025.152944.1338

[25] Sánchez, A., Varum, H., Martins, T., Fernández, J. (2022). Mechanical properties of adobe masonry for the rehabilitation of buildings. Construction and Building

Materials, 333: 127330. https://doi.org/10.1016/j.conbuildmat.2022.127330
[26] Rakesh, S., Keshava, M. (2019). A study on embodied energy of recycled aggregates obtained from processed demolition waste. In National Conference on Recent Trends in Architecture & Civil Engineering Towards Energy Efficient and Sustainable Development, NIT Tiruchirapalli.
[27] Andrew, A. (2003). Embodied energy and CO2 coefficients for NZ building materials. Centre for Building Performance Research. https://www.wgtn.ac.nz/architecture/centres/cbpr/resources/pdfs/ee-co2_report_2003.pdf.